A

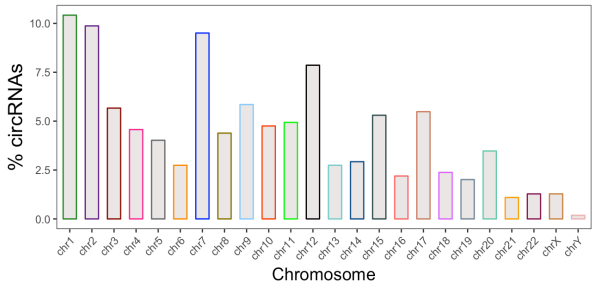

B

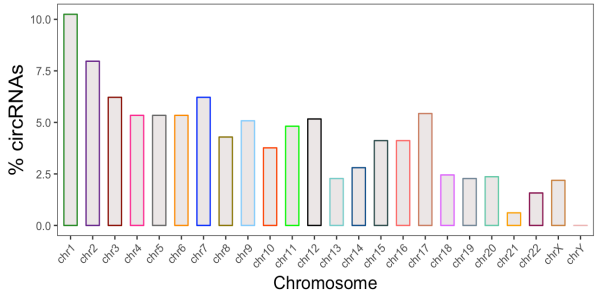

Suppl. Fig. S1. Chromosome distribution of the DE circRNAs. (A) and (B) Chromosome distribution of the DE circRNAs from total RNA dataset (A) and circRNA enriched dataset (B).

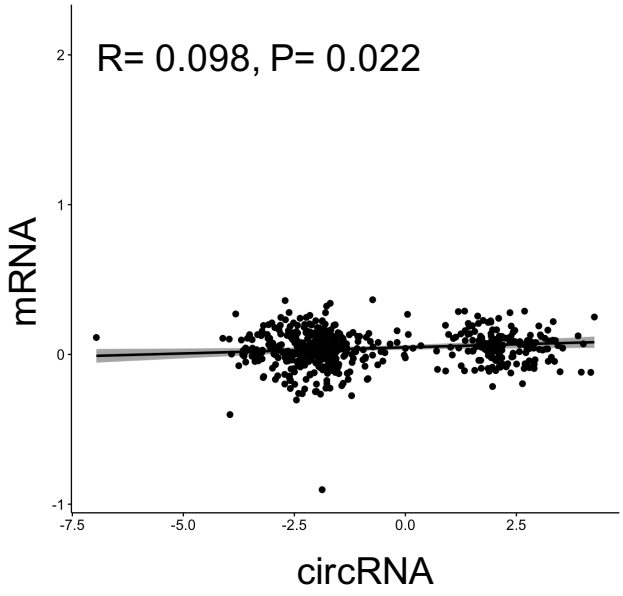

Suppl. Fig. S2. Correlation of DE circRNAs with their host mRNA. The DE circRNAs show a significantly positive correlation with their host mRNA.

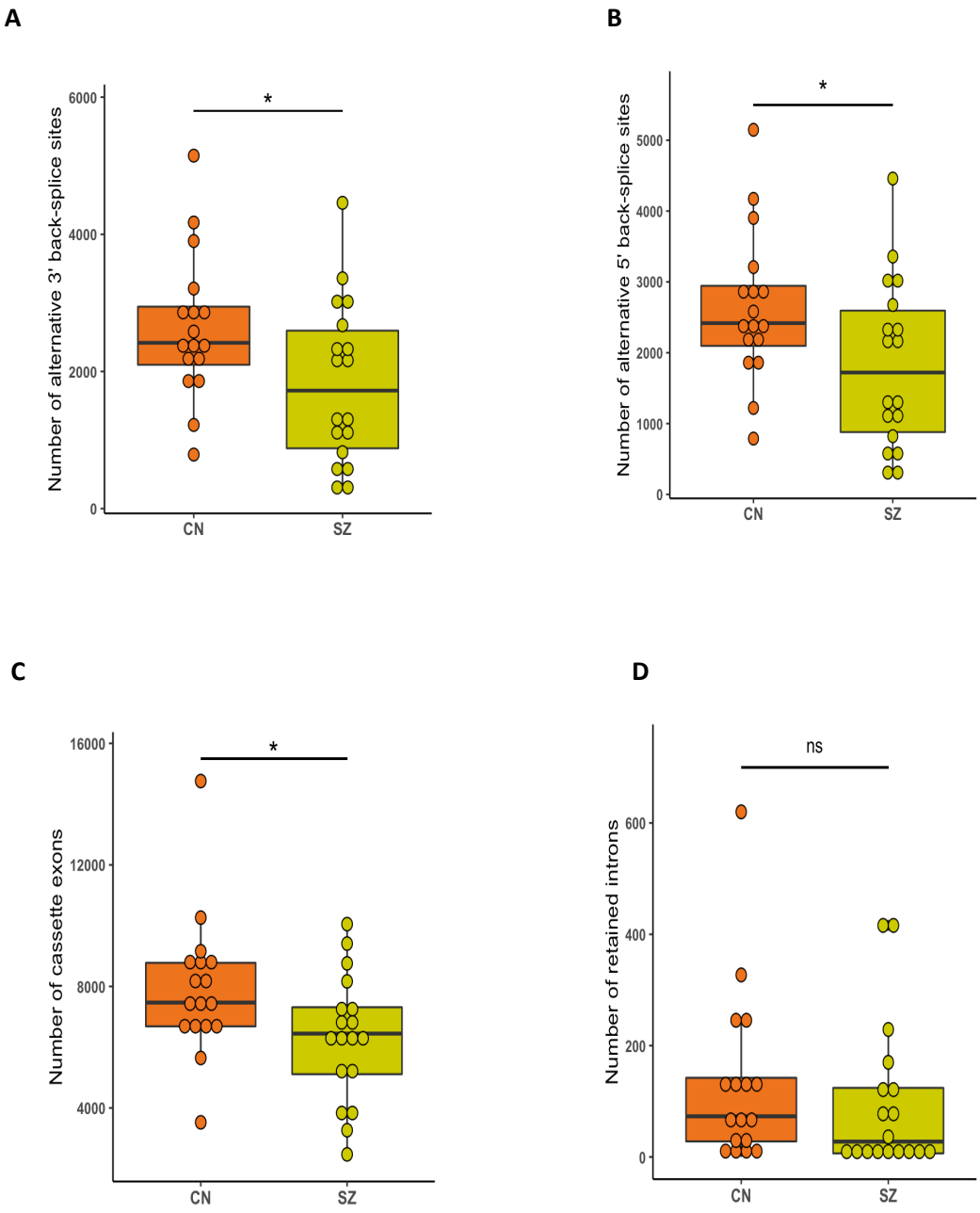

Suppl. Fig. S3. Identification of four alternative splicing events in circular RNAs. (A)(B)(C)(D) Four types of alternative splicing events including alternative 3' splice sites (A), alternative 5' splice sites (B), cassette exons (C), retained introns (D) were predicted and counted for unique events for two diagnosis groups. The statistical test was performed using t-test (two-tailed). *$P < 0.05$.

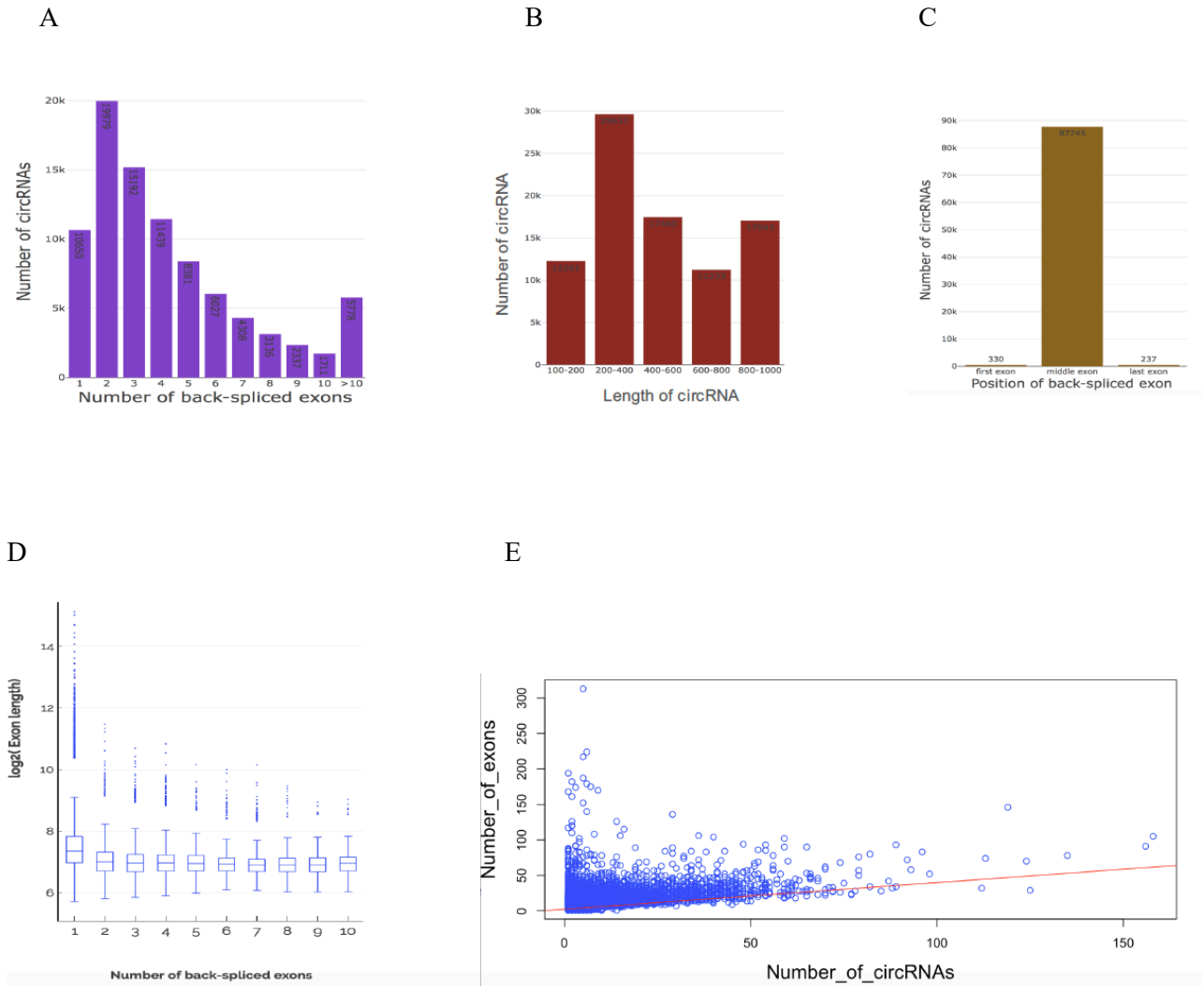

Suppl. Fig. S4. Features of exons producing circRNAs. (A) Number of exons per circRNA. (B) Exonic length of circRNA transcripts. (C) Position of circularized exons in circRNAs. (D) Plot of back-spliced exons against their length. (E) Correlation between number of circRNAs and number of their exons using Kendall correlation.

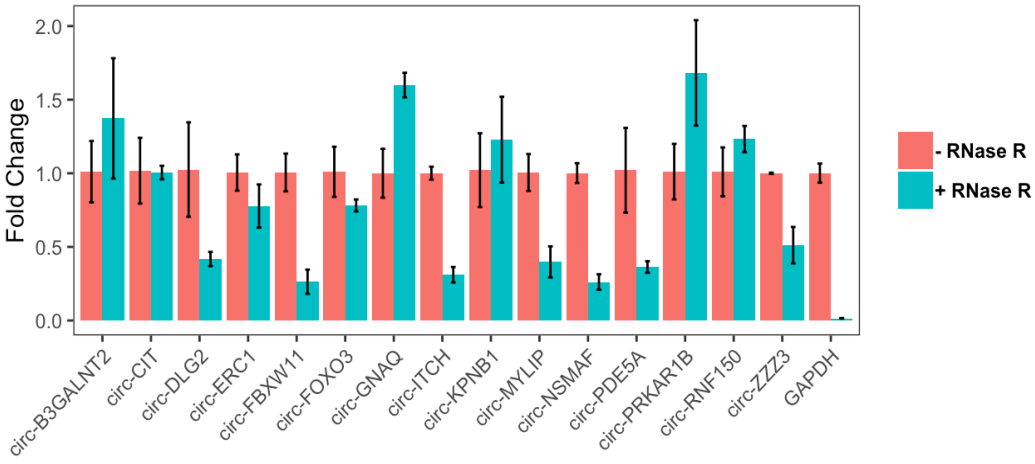

Suppl. Fig. S5. Validation of circRNA resistance to RNase R using qRT-PCR. RNA isolated from BA46 region of brain was treated with RNAse R (+ RNase) or mock treated (-RNase R). Data are mean ± s.d. with 3 technical replicates. GAPDH was used as a control.

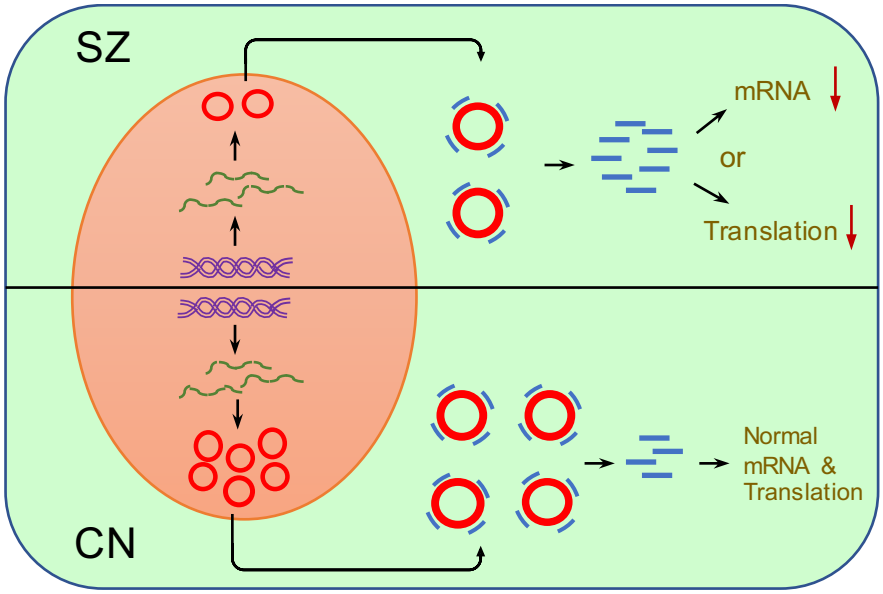

Suppl. Fig. S6. Proposed regulatory model of circRNAs-miRNA association in SZ. Global downregulation of circRNAs in SZ reduces sponging of miRNA which results in bioavailability of the miRNA. Subsequently, target mRNA levels decrease or they are prevented from translation. In contrast, healthy individuals produce normal amount of circRNAs which fine-tunes miRNA expression, leading to normal mRNA levels and translation.